

Early phase simultaneous multi-band observations of Type II supernova SN 2024ggi with Mephisto

Xinlei Chen^a, Brajesh Kumar^{a,*}, Xinzong Er^a, Helong Guo^a, Yuan-Pei Yang^a, Weikang Lin^a, Yuan Fang^a, Guowang Du^a, Chenxu Liu^a, Jiewei Zhao^b, Tianyu Zhang^a, Yuxi Bao^a, Xingzhu Zou^a, Yu Pan^a, Yu Wang^a, Xufeng Zhu^a, Kaushik Chatterjee^a, Xiangkun Liu^a, Dezi Liu^a, Edoardo P. Lagioia^a, Geeta Rangwal^a, Shiyuan Zhong^a, Jinghua Zhang^a, Jianhui Lian^a, Yongzhi Cai^{c,d,e}, Yangwei Zhang^a and Xiaowei Liu^a

^aSouth-Western Institute for Astronomy Research, Yunnan University, Kunming, 650504, Yunnan, P.R. China

^bDepartment of Astronomy, Yunnan University, Kunming, 650504, Yunnan, P.R. China

^cYunnan Observatories, Chinese Academy of Sciences, Kunming, 650216, Yunnan, P.R. China

^dKey Laboratory for the Structure and Evolution of Celestial Objects, Chinese Academy of Sciences, Kunming, 650216, Yunnan, P.R. China

^eInternational Centre of Supernovae, Yunnan Key Laboratory, Kunming, 650216, Yunnan, P.R. China

ARTICLE INFO

Keywords:

Supernova: SN 2024ggi
Core-collapse supernovae
Red supergiant stars
Circumstellar matter
Observational astronomy

ABSTRACT

We present early-phase good cadence simultaneous multi-band (*ugr*, *vrz*-bands) imaging of nearby supernova SN 2024ggi, which exploded in the nearby galaxy, NGC 3621. A quick follow-up was conducted within less than a day after the explosion and continued \sim 23 days. The *ugr*-band light curves display a rapid rise (\sim 1.4 mag day $^{-1}$) to maximum in \sim 4 days and absolute magnitude $M_g \sim$ 17.75 mag. The post-peak decay rate in redder bands is \sim 0.01 mag day $^{-1}$. Different colors (e.g., $u - g$ and $v - r$) of SN 2024ggi are slightly redder than SN 2023ixf. A significant rise (\sim 12.5 kK) in black-body temperature (optical) was noticed within \sim 2 days after the explosion, which successively decreased, indicating shock break out inside a dense circumstellar medium (CSM) surrounding the progenitor. Using semi-analytical modeling, the ejecta mass and progenitor radius were estimated as $1.2 M_{\odot}$ and \sim 550 R $_{\odot}$, respectively. The archival deep images (*g, r, i, z*-bands) from the Dark Energy Camera Legacy Survey (DECaLS) were examined, and a possible progenitor was detected in each band (\sim 22–22.5 mag) and had a mass range of 14–17 M $_{\odot}$.

1. Introduction

In recent years, Type II supernovae (SNe) have drawn substantial attention from the time domain community due to their very early detection after the explosion. These events are a subclass of core-collapse supernovae (CCSNe) and originate from the red supergiant (RSG) progenitors (zero-age main-sequence mass range \gtrsim 8–25 M $_{\odot}$) at the end stage of their evolution (Smartt, 2009, 2015). The spectro-photometric properties led to further subclassification of Type II events (e.g., IIP, IIL, IIb, and IIn), but the presence of Balmer lines in their spectra is a common feature (Filippenko, 1997). The light curve evolution is mainly governed by the hydrogen envelope mass retained before the explosion and the explosion energy (Dessart et al., 2013). The earliest post-explosion observation (minutes–hours to days) is crucial as it retains information about the shock-breakout (SBO)/shock-cooling emission and the pre-existing circumstellar medium (CSM) surrounding the progenitor (see Waxman and Katz, 2017; Morozova et al., 2018; Moriya et al., 2018).

The presence or absence of CSM strongly influences the appearance of light curves and spectral features, especially during the early epochs (Chevalier and Irwin, 2011). SBO

is revealed in the form of ultraviolet (UV)/ X-ray radiation immediately after the gravitational collapse of the stellar core, lasting for minutes to several hours. The propagating shock finally breaks out of the stellar surface and ionizes the surrounding CSM, which consequently appears as “flash” features in the spectra (Quimby et al., 2007; Gal-Yam et al., 2014; Yaron et al., 2017). Subsequently, shock-cooling emission occurs in UV/optical wavelengths, where the radiation is driven by photons escaping from deeper layers in the expanding envelope. The duration of shock-cooling may survive several days, depending upon the CSM composition. Due to the short timescale, the early phase observations of Type II are very limited, and only a handful of events have been adequately monitored and studied in detail, e.g., SN 2013fs (Yaron et al., 2017), SN 2016gkg (Tartaglia et al., 2017), SN 2018zd (Zhang et al., 2020; Hiramatsu et al., 2021), SN 2023ixf (Li et al., 2024; Teja et al., 2023; Hosseinzadeh et al., 2023b; Zhang et al., 2023). Investigating multi-band early phase light curves with a good cadence is important to determine various parameters of the progenitor (see Rabinak and Waxman, 2011; Hosseinzadeh et al., 2023b, and references therein).

SN 2024ggi (ATLAS24fsk, GOTO24aig, PS24brj) is another nearby event after last year’s SN 2023ixf (Itagaki, 2023), discovered in the early phase after the explosion and provides an excellent opportunity to investigate the observational properties comprehensively, including its progenitor.

*Corresponding author

 brajesh@ynu.edu.cn (B. Kumar); xer@ynu.edu.cn (X. Er); x.liu@ynu.edu.cn (X. Liu)
ORCID(s):

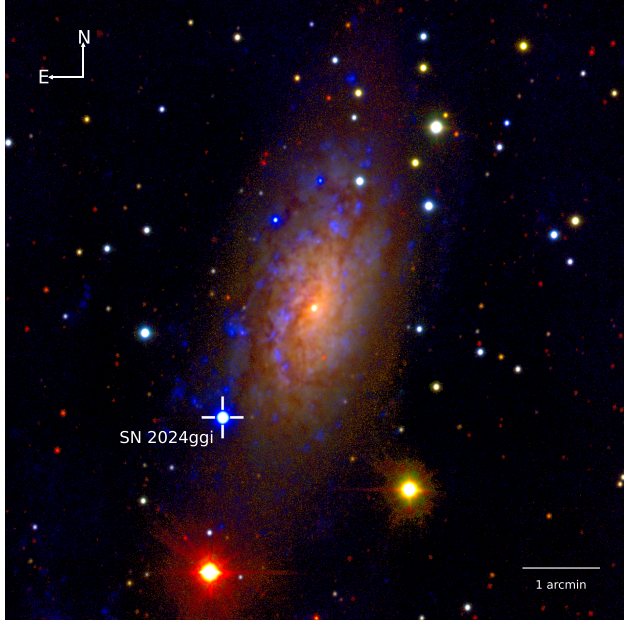


Figure 1: SN 2024ggi in the spiral galaxy NGC 3621 is marked. This color composite image is created using the several night stacked frames of the Mephisto three bands (u, g, i). Colors are adjusted to enhance the features. The SN is indicated with a cross-hair, and the displayed image size is $\sim 8' \times 8'$.

In this paper, we present early-phase multi-band simultaneous imaging of SN 2024ggi. The SN was discovered (Tonry et al., 2024; Srivastav et al., 2024) in NGC 3621 on MJD 60411.14 (UT 2024 April 11.14) by the ATLAS survey group with a discovery magnitude of 18.915 (orange-ATLAS). Fast rising was confirmed in further monitoring (Chen et al., 2024). The early spectra taken within a few hours suggest a type II SN with flash features and the redshift $z_s = 0.002435$ (Hoogendam et al., 2024; Zhai et al., 2024). Using the Gravitational-wave Optical Transient Observer (GOTO; Steeghs et al., 2022) imaging, Killestein et al. (2024) put a strong constraint on the explosion epoch MJD 60410.80, which is consistent as estimated by Jacobson-Galán et al. (2024). We have adopted it further in this paper.

Recently, Jacobson-Galán et al. (2024) investigated the UV/optical/NIR observations and early spectroscopy of SN 2024ggi. Their first spectrum exhibits prominent narrow emission lines (H α , He I, C III, and N III), likely because of the photo-ionization of dense, optically thick CSM. High-resolution spectroscopy reveals early flash-ionization lines (Pessi et al., 2024). X-ray emission at SN 2024ggi location was also detected in a few days after the discovery by different X-ray missions, (Margutti and Grefenstette, 2024; Zhang et al., 2024) which suggests SN shock interaction with the dense medium.

In Section 2, we provide the observation and data analysis of Mephisto's follow-up. Section 3 discusses the light curve properties, including the color and bolometric light curve evolution. The progenitor properties and summary are presented in Section 4 and Section 5, respectively.

2. Mephisto observations and data reduction

The photometric observations of SN 2024ggi were initiated with the 1.6 m **M**ulti-channel **P**hotometric **S**urvey **T**elescope (Mephisto, Liu et al. in preparation) immediately after receiving the TNS notice. However, due to limitations of the southern sky target and weather, the first frame was obtained at MJD = 60411.64 (UT 2024 April 11.64). After detecting SN 2024ggi in our initial images, we continued monitoring the target until its availability in the sky. The SN was followed up on consecutive nights whenever the conditions permitted. A stacked image of Mephisto frames marking the SN location is shown in Fig. 1.

It is important to highlight that Mephisto is a wide-field multi-channel telescope, the first of its type worldwide. The facility is located at Lijiang Observatory (IAU code: 044) of Yunnan Astronomical Observatories, Chinese Academy of Sciences (CAS), with longitude $100^{\circ}01'48''$ East, latitude $26^{\circ}41'42''$ North and altitude 3200m (more details about the site can be found in Wang et al., 2019). The South-Western Institute for Astronomy Research, Yunnan University, operates the Mephisto facility. The Mephisto is presently in commissioning phase. However, it is already contributing with good quality scientific data (see, e.g. Chen et al., 2024). It is equipped with three-channel CCD cameras and is capable of performing simultaneous observations in ugr or vrz optical bands at each pointing. While the mosaic cameras are in the final stage of manufacturing, the commissioning observations are performed with two Andor Technology single-chip (e2v CCD231-C6 6144 \times 6160 sensor) CCD cameras for the blue (uv) and yellow (gr) channels, respectively. The red channel (iz) is equipped with another single-chip type (e2v CCD 290-99 9216 \times 9232, $10\mu\text{m}$ sensor). Thus, the spatial resolution of images in the red channel slightly differs from that of the yellow and blue channels. The wavelength coverage of the u, v, g, r, i, z filters are $320 - 365, 365 - 405, 480 - 580, 580 - 680, 775 - 900$ and $900 - 1050$ nm, respectively (c.f. Fig. 7).

Since the location of SN 2024ggi is in the Southern Hemisphere ($\text{Dec} = -32.84^{\circ}$), there is a limitation for Mephisto to observe the source full night and only about one-hour observation could be performed. We allocated all the possible observing time for SN 2024ggi during the first week after its discovery. The two sets of filters, ugr and vrz , were executed consecutively.

The raw frames were pre-processed (bias subtraction, flat fielding, and cosmic ray removal) using a pre-processing pipeline developed for the Mephisto (Fang Y. et al. in preparation). Point spread function (PSF) photometry was performed on the cleaned images to get the instrumental magnitudes. We utilized the Gaia XP spectra of non-variable stars to perform photometric calibration. Because Gaia XP spectra exhibit systematic errors that depend on magnitude, color, and extinction, particularly at wavelengths below 400 nm, we used the corrected Gaia XP spectra from Huang et al. (2024). The wavelength coverage of Gaia XP spectra is from 336 to 1020 nm, which does not fully cover our u or z -bands. Thus, we extrapolated the spectra for the u (336 –

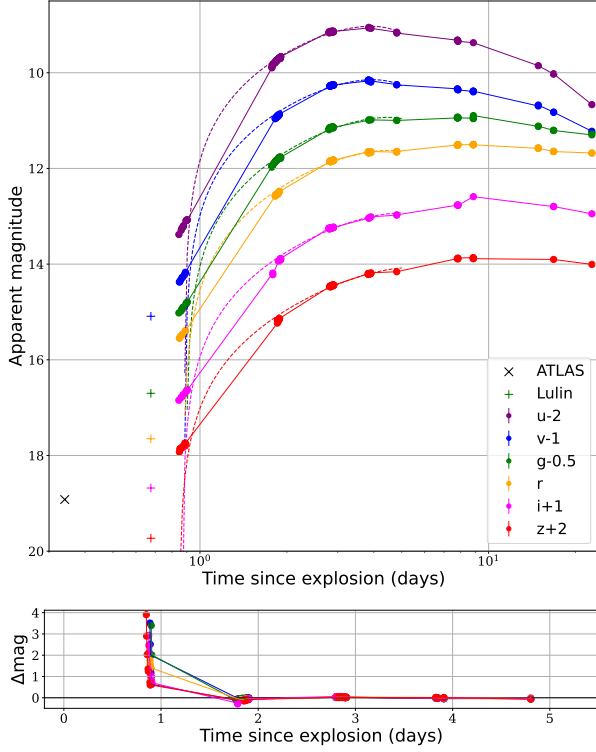


Figure 2: Top panel: *uvgriz*-band light curve evolution of SN 2024ggi. Indicated offsets have been applied to the apparent magnitudes for clarity. The cross marks the time and magnitude of discovery by ATLAS (Tonry et al., 2024; Srivastav et al., 2024), plus symbols indicate the early observations by Lulin observatory (Chen et al., 2024). One should notice that the filter systems used by ATLAS and Lulin differ from those used by Mephisto. The dotted lines are the fitting light curves using a single power-law model (see Section 3.1). Bottom panel: The residuals between the fitting light curves and the observations in six bands by Mephisto.

364 nm) and *z*-band. We computed each band’s synthetic magnitude in the AB system by convolving the spectra with the transmission efficiency. We calculated the difference between the instrumental and synthetic magnitude Δm for the non-variable stars and used the median Δm to calibrate our photometric measurements. The possible flux contamination due to the host galaxy has not been removed as the SN is very bright, and we consider that host flux has a minimal effect at this stage.

The foreground extinction from the Milky Way in the line of sight of SN 2023ixf is $E(B - V)_{\text{MW}} = 0.070$ mag (Schlafly and Finkbeiner, 2011). For the extinction from the host galaxy, Jacobson-Galán et al. (2024) obtained $E(B - V)_{\text{host}} = 0.084 \pm 0.018$ mag by calculating the equivalent widths (EWs) of NaI D2 and D1. According to the total extinction of $E(B - V)_{\text{total}} = 0.154 \pm 0.018$ mag and the extinction law of Fitzpatrick (1999) ($R_V = 3.1$), we finally obtained the extinction values of 0.762, 0.695, 0.496, 0.390, 0.248, and 0.202 mag for the *u, v, g, r, i, z*-bands, respectively. An estimate for the distance of the host galaxy NGC 3621 over different methods (Cepheids, TRGB, and

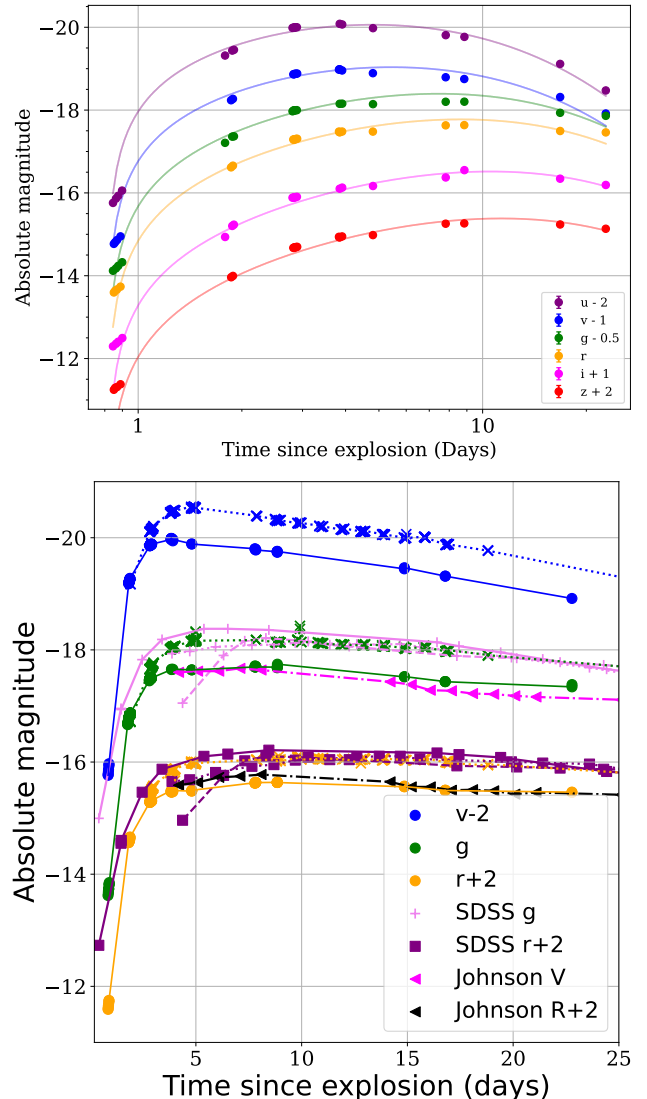


Figure 3: Top panel: Fitting the shock cooling model of (Hosseinzadeh et al., 2017) to the multi-band light curves of SN 2024ggi. Bottom panel: The multiple-band light curves of SN 2024ggi (solid) and other Type II SNe. The blue, green, and orange points show observations with Mephisto filters (*v, g, r*). SN 2023ixf: crosses and dotted lines; SN 2020pni: pluses, squares and solid lines; SN 2014G: pluses, squares and dotted lines; SN 2018zd: pluses, squares and dashed lines; SN 2013fs: triangles and dot-dashed line. The other color points show observations with filters of SDSS *g, r* (violet and purple) or Johnson *V, R* (magenta and black).

Tully-Fisher) is adopted which is 6.73 Mpc. The distance module is 29.14.

3. Results

3.1. Light curve properties

In this section, we examined the light curve properties of SN 2024ggi, compared with other similar types of events,

Table 1

The best fitting value of the shock cooling model (Hosseinzadeh et al., 2017) using package Hosseinzadeh et al. (2023a). The ejecta mass is a combination $f_\rho M$, which always appears together in the shock cooling formalism.

Parameter	Variable	Result
Shock speed (10^8 cm/s)	v_s	$5.60^{+0.09}_{-0.13}$
Envelope mass (M_\odot)	M_{env}	$1.66^{+0.03}_{-0.03}$
Ejecta mass (M_\odot)	$f_\rho M$	$1.2^{+0.3}_{-0.2}$
Progenitor radius (10^{13} cm)	R	$3.81^{+0.07}_{-0.07}$
Explosion epoch (day)	t_0	$60411.61^{+0.0001}_{-0.0001}$

and also estimated different parameters by modeling the light curves. In Fig. 2, the $uvgriz$ -band light curves of SN 2024ggi observed by Mephisto are displayed. It is interesting to note that the u and v -band reached a peak within 4 days and then started to decrease. We used a fireball model to fit the initial five days of our photometric data points (dotted lines in the figure) to understand the light curve evolution at the early phase. It should be noted that the black-body temperature decreases rapidly after 2 days; however, in this fitting, we assume that the temperature is constant. The flux is expressed as $f \propto (t - t_0)^2$ (Hosseinzadeh et al., 2023b). The fitting curves can represent the observed light curves from the second to the fifth day. However, such a fitting yields the first light epoch as MJD 60411.65, which is about 11 hours later than the discovery epoch by ATLAS and GOTO observation (see Section 1).

The residual magnitudes for the first five days from the fitting curves are shown in the bottom panel of Fig. 2. Even with our observations from the first day, a relatively large inconsistency can be seen in all six bands. During the first day, the difference between the z and v -band reached 4 magnitudes. It is clear that a single power law could not describe the light curve in any band in the early phase. The disagreement between the observed and fitting first light epoch was also noticed in the case of SN 2023ixf (Hosseinzadeh et al., 2023b), and several explanations were provided, such as the rising light curve is due to an eruption or instability activity in the progenitor before the gravitational collapse of the core (mass loss) and/or strong influence of CSM interaction. To constrain the progenitor properties and explosion parameters of SN 2024ggi, the Light Curve Fitting package (Hosseinzadeh et al., 2023a) was used to fit observed photometry. The estimated parameters are listed in Table 1, and the fitted models are displayed in Fig. 3 (top panel).

In Fig. 3 (bottom panel), we compare the multiple band light curves of SN 2024ggi with other well-studied events. Here, only those events were considered that were discovered early with flash features, such as SNe 2023ixf, 2013fs, 2014G, and 2018zd. It can be clearly seen that SN 2024ggi evolved rapidly and reached maximum light within 4 days. The peak absolute magnitude is -17.75 in g -band, while SN 2023ixf reached the peak after 5 days, with a peak magnitude of $M_g = -18.43$. Both are toward the brighter end of normal Type II SNe (16.74 mag, Anderson et al., 2014)

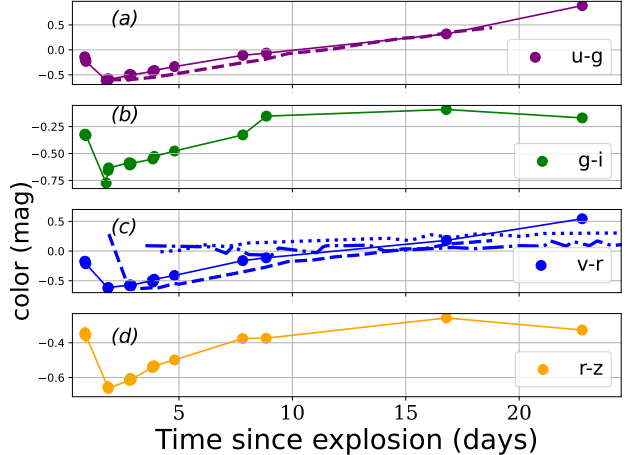


Figure 4: The color evolution of SN 2024ggi in the beginning 18 days. For comparison, the color curves of several same types of SNe are over-plotted: SN 2023ixf obtained from Mephisto (dashed), SN 2013fs (dotted) and SN 2018zd (dot-dashed). The filters of SN 2013fs and SN 2018zd are Johnson V and R .

and (16.89 mag, Galbany et al., 2016). It is also notable that the rise time (in u , v -bands) of ~ 4 days in SN 2024ggi is significantly shorter than the average peak rise time ~ 10 days of normal Type II events (Valenti et al., 2016). The r , i , z light curves rise to the maximum 8.5 ± 0.5 days after the explosion.

3.2. Color and pseudo-bolometric light curve evolution

The color evolution of SNe provides substantial information about the temperature, chemical composition, and shock interaction with CSM in the vicinity of the progenitor. Two-fold color evolution has been observed in normal Type II events. As the surface temperature decreases, the color indices gradually approach the redder side for the first few weeks, which later becomes shallower (Galbany et al., 2016). In large sample studies, a moderate correlation has been observed between the different phase color indices and the explosion energy and ^{56}Ni mixing (Martinez et al., 2022). The multicolor information of CSM interacting SNe is less, especially in the early phase. The CSM interacting events display a reversal in UV-optical colors from red-blue to blue-red in about 5 days after the explosion (Zhang et al., 2020; Hiramatsu et al., 2021).

Taking advantage of simultaneous Mephisto imaging (cf. ugr and vrz), we investigated the four colors ($u - g$, $g - i$, $v - r$, $r - z$) of SN 2024ggi. The intrinsic colors are displayed in Fig. 4. It is evident that the SN became bluer rapidly in all colors during the first two days. The color indices $u - g$, $g - i$, $v - r$, $r - z$ changed from ~ -0.4 , -0.3 , -0.1 , -0.35 mag to ~ -0.6 , -0.75 , -0.6 , -0.7 mag, respectively in this period. The $u - g$ and $v - r$ colors became redder after 2 days and continued until the observations. However, there is a reversal in the evolution of $g - i$ and $r - z$ colors. In panel

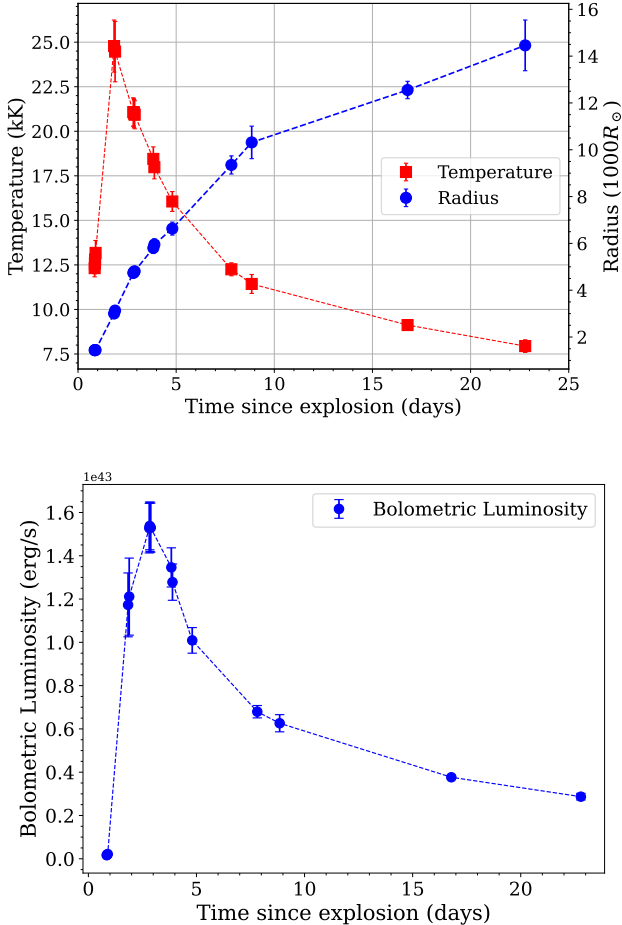


Figure 5: Top panel: the evolution of BB temperature and radius of SN 2024ggi. Bottom panel: the bolometric luminosity.

(c) of Fig. 4, the $v - r$ color of SNe 2013fs, 2018zd, 2023ixf (where flash features were identified) is over-plotted for a comparison. Fig. 4 indicates that the color evolution rate in SN 2023ixf was faster than other events in the beginning, and both SN 2024ggi and SN 2023ixf are bluer than other SNe. After ~ 2.5 days, all colors gradually became redder. SN 2024ggi has a higher excess in all color indices. The initial blue color also signifies high temperature and lines of flash-ionization (Jacobson-Galán et al., 2024; Pessi et al., 2024).

The pseudo-bolometric light curve of SN 2024ggi was constructed using SuperBol (Nicholl, 2018). The extinction corrected $uvgriz$ magnitudes and distance 6.73 Mpc were used as input parameters. Here, it is emphasized that the UV/NIR contributions were not included in deriving the bolometric magnitudes, but they may have a reasonable contribution in some cases like SN 2023ixf (Jacobson-Galán et al., 2024; Teja et al., 2023; Zimmerman et al., 2023). The pseudo-bolometric light curve is plotted in Fig. 5, which reached to maximum on day 2.6 ± 0.2 with bolometric luminosity of $(1.54 \pm 0.12) \times 10^{43}$ erg s⁻¹. The temperature and radius parameters that resulted in the black body fit

are shown in Fig. 5. It is worth noting that the temperature evolution, in the beginning, does not follow the usual trend of normal Type II SNe where temperature cools rapidly with increasing photospheric radius after the shock break out (Falk and Arnett, 1977). In a day, the temperature reached from 12500 K to 25000 K. A similar rise was noticed by Jacobson-Galán et al. (2024) in SN 2024ggi and also in SN 2023ixf (Zimmerman et al., 2023) (although UV flux was included). Such features of temperature evolution are indicative of a possible shock break out inside a compact and dense CSM surrounding the progenitor (Moriya et al., 2018; Hiramatsu et al., 2021; Li et al., 2024; Zhang et al., 2020).

4. Possible progenitor of SN 2024ggi

A reasonable number of direct progenitor detections of Type II SNe have been possible in recent years thanks to high-resolution images from space and ground-based facilities (see, e.g. Smartt, 2009, 2015; Tartaglia et al., 2017). Several studies of the SN 2023ixf progenitor were made due to its proximity to the Earth (Kilpatrick et al., 2023; Liu et al., 2023; Soraisam et al., 2023). As the RSG progenitors have a large mass range, any new possible identification is important to better constrain the mass limit.

Similar to SN 2023ixf, a possible progenitor has been identified at the location of SN 2024ggi in the images of the Dark Energy Camera Legacy Survey Data Release 10 (DECALS¹). We performed photometry for the progenitor in the g, r, i , and z band images taken by DECam (Honscheid and DePoy, 2008). Because the z -band image has the highest quality, i.e., PSF and signal-to-noise ratio, the SWARP² was used to align the astrometric solutions of the g, r and i -band images in reference to the z -band image. Then we used the dual-image mode of SExtractor³ to do a series of aperture photometry for the progenitor, with aperture diameters from 1.5 to 46.5 pixels for each band image. We chose the aperture with the highest signal-to-noise ratio as the best aperture and performed aperture correction for the corresponding magnitude using the growth curve. A clear detection in g, r, i, z -bands has been noticed, and the estimated g, r, i, z magnitudes are $22.51 \pm 0.02, 22.74 \pm 0.02, 22.73 \pm 0.03, 21.90 \pm 0.02$, respectively. The estimated magnitudes are similar to Yang et al. (2024) within error limits. It should be noted that the possible progenitor has also been identified in archival images of the Hubble Space Telescope (HST) and VISTA Hemisphere Survey (Srivastav et al., 2024; Pérez-Fournon et al., 2024). However, the source is resolved into two sources in the HST F814W band (Srivastav et al., 2024).

We used the PARSEC⁴ stellar evolutionary isochrones (Bressan et al., 2012) to estimate the mass of the progenitor. We present the progenitor on the color-magnitude diagram of g and z bands (Fig. 6). Again, the same extinction as

¹<https://www.legacysurvey.org/decals/>

²<https://www.astromatic.net/software/swarp/>

³<https://www.astromatic.net/software/sextar/>

⁴<http://stev.oapd.inaf.it/cgi-bin/cmd/>

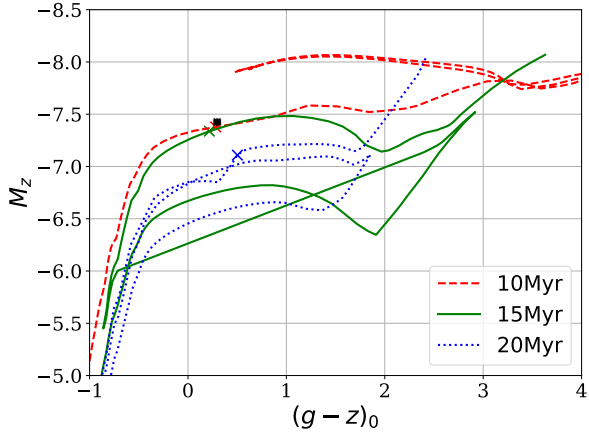


Figure 6: The color-magnitude diagram of 10, 15 and 20 Myr PARSEC stellar evolutionary isochrones with metallicity of $Z = 0.025$ (red dashed), $Z = 0.01$ (green solid), $Z = 0.001$ (blue dotted) along with our progenitor candidate. The black square is the color-magnitude position measured from DECaLS images. The red, green, and blue cross symbols of initial mass 17, 14, and $11 M_{\odot}$, respectively.

mentioned in Section 2 is used here. The isochrones that match the measurement best have an age of ~ 10 (red) or 15 (green) Myr, with an initial mass of 17 or 14 M_{\odot} , a metallicity of $Z = 0.025$ or $Z = 0.01$. As a comparison, the progenitor of the SN 2023ixf has been identified as a red super-giant as well. The mass estimate of the progenitor covers a large range from $\sim 20 M_{\odot}$ (e.g., using CFHTLS data, Liu et al., 2023) to a smaller $\sim 15 - 17 M_{\odot}$ (e.g., using a BPASS model with HST data, Eldridge et al., 2017; Jencson et al., 2023).

5. Summary

This work presents a good cadence of early light curves (between less than a day to about 24 days after explosion) of SN 2024ggi, a nearby Type II SN in the galaxy NGC 3621 (~ 6.73 Mpc). Simultaneous multi-band (ugr , vri) photometric observations were performed with the 1.6m Multi-channel Photometric Survey Telescope (Mephisto), which is equipped with three channels: Blue (uv), Yellow (gr) and Red (iz). The multi-band color information was used to infer the shock break out, color evolution, and CSM interaction. The $u - g$, $g - i$, $v - r$, and $r - z$ color evolution of SN 2024ggi demonstrate a blue excess in the beginning (two days after first light). Later, $u - g$ and $v - r$ colors display a redward evolution until day ~ 23 (post-explosion). However, $g - i$ and $r - z$ are turning bluer again after ~ 15 days. SN 2024ggi reached to maximum $M_g = -17.75$ mag on day 4 post-explosion, which is towards the bright side in comparison to normal Type II events. The black-body (optical) temperature evolution appears interesting. It increases from 12500 K to 25000 K in 2 days after the explosion and thereafter decreases (Section 3.2). Such characteristics have also been noticed in SN 2018zd and SN 2023ixf.

The explosion parameters and progenitor properties were estimated by modeling the light curves with a shock-cooling model (see Section 3.1). The comprehensive photometric properties of SN 2024ggi indicate that pure shock-cooling emission may not be attributed to them. Rather, a delayed shock-breakout from a dense CSM is favorable, as also witnessed in SN 2023ixf.

We examined the archival images of Dark Energy Camera Legacy Survey Data Release 10 (DECaLS) to search for the possible progenitor of SN 2024ggi. A progenitor candidate was identified in g , r , i and z -bands with magnitudes 22.51 ± 0.02 , 22.74 ± 0.02 , 22.73 ± 0.03 , 21.90 ± 0.02 , respectively. However, in HST images, two sources were resolved at the SN location. The best-fitted stellar evolutionary isochrones (solar metallicity) to the extinction-corrected magnitudes indicate a possible progenitor with a mass range of $14 - 17 M_{\odot}$ (see, Section 4). Although a more robust progenitor model can better constrain the initial mass of SN 2024ggi, our estimated mass range is towards the lower mass limit of RSGs, as found in the direct identification of Type II progenitors.

It is evident from the observations of nearby SN 2024ggi and SN 2023ixf that prompt and good cadence data is essential to study on various aspects of the progenitor, explosion, and surrounding CSM. A coordinated multi-wavelength follow-up is important. Therefore, the upcoming and existing facilities will play a pivotal role in this regard. The Mephisto facility is expected to be equipped with the three mosaic CCD cameras by the end of 2024. The unique feature of simultaneously imaging the particular patch of sky in three bands (ugr and vri) will provide a unique opportunity to discover transient sources on the basis of their colors and successive monitoring.

Acknowledgments

We would like to thank Griffin Hosseinzadeh for the help with the light curve fitting code. Mephisto is developed at and operated by the South-Western Institute for Astronomy Research of Yunnan University (SWIFAR-YNU), funded by the “Yunnan University Development Plan for World-Class University” and “Yunnan University Development Plan for World-Class Astronomy Discipline”. The authors acknowledge support from the “Science & Technology Champion Project” (202005AB160002) and from two “Team Projects” – the “Top Team” (202305AT350002) and the “Innovation Team” (202105AE160021), all funded by the “Yunnan Revitalization Talent Support Program”. Y.-Z. Cai is supported by the National Natural Science Foundation of China (NSFC, Grant No. 12303054), the Yunnan Fundamental Research Projects (Grant No. 202401AU070063) and the International Centre of Supernovae, Yunnan Key Laboratory (No. 202302AN360001). We acknowledge the observers and technical support staff for helping with the observations. BK thanks J. Craig Wheeler and Avinash Singh for important comments and discussions on the manuscript.

References

- Anderson, J.P., González-Gaitán, S., Hamuy, M., Gutiérrez, C.P., Stritzinger, M.D., Olivares E., F., Phillips, M.M., Schulze, S., Antezana, R., Bolt, L., Campillay, A., Castellón, S., Contreras, C., de Jaeger, T., Folatelli, G., Förster, F., Freedman, W.L., González, L., Hsiao, E., Krzeminski, W., Krisciunas, K., Maza, J., McCarthy, P., Morrell, N.I., Persson, S.E., Roth, M., Salgado, F., Suntzeff, N.B., Thomas-Osip, J., 2014. Characterizing the V-band Light-curves of Hydrogen-rich Type II Supernovae. *Astrophys Jour* 786, 67. doi:10.1088/0004-637X/786/1/67, arXiv:1403.7091.
- Bressan, A., Marigo, P., Girardi, L., Salasnich, B., Dal Cero, C., Rubele, S., Nanni, A., 2012. PARSEC: stellar tracks and isochrones with the PAدوا and TRieste Stellar Evolution Code. *Mon Not R Astron Soc* 427, 127–145. doi:10.1111/j.1365-2966.2012.21948.x, arXiv:1208.4498.
- Chen, P., Gal-Yam, A., Sollerman, J., Schulze, S., Post, R.S., Liu, C., Ofek, E.O., Das, K.K., Fremling, C., Horesh, A., Katz, B., Kushnir, D., Kasliwal, M.M., Kulkarni, S.R., Liu, D., Liu, X., Miller, A.A., Rose, K., Waxman, E., Yang, S., Yao, Y., Zackay, B., Bellm, E.C., Dekany, R., Drake, A.J., Fang, Y., Fynbo, J.P.U., Groom, S.L., Helou, G., Irani, I., Jegou du Laz, T., Liu, X., Mazzali, P.A., Neill, J.D., Qin, Y.J., Riddle, R.L., Sharon, A., Strotjohann, N.L., Wold, A., Yan, L., 2024. A 12.4-day periodicity in a close binary system after a supernova. *Nature* 625, 253–258. doi:10.1038/s41586-023-06787-x, arXiv:2310.07784.
- Chevalier, R.A., Irwin, C.M., 2011. Shock Breakout in Dense Mass Loss: Luminous Supernovae. *Astrophys Jour Lett* 729, L6. doi:10.1088/2041-8205/729/1/L6, arXiv:1101.1111.
- Dessart, L., Hillier, D.J., Waldman, R., Livne, E., 2013. Type II-Plateau supernova radiation: dependences on progenitor and explosion properties. *Mon Not R Astron Soc* 433, 1745–1763. doi:10.1093/mnras/stt861, arXiv:1305.3386.
- Eldridge, J.J., Stanway, E.R., Xiao, L., McClelland, L.A.S., Taylor, G., Ng, M., Greis, S.M.L., Bray, J.C., 2017. Binary Population and Spectral Synthesis Version 2.1: Construction, Observational Verification, and New Results. *Publ of the Astron Soc of Australia* 34, e058. doi:10.1017/pasa.2017.51, arXiv:1710.02154.
- Falk, S.W., Arnett, W.D., 1977. Radiation Dynamics, Envelope Ejection, and Supernova Light Curves. *Astrophys Jour Suppl* 33, 515. doi:10.1086/190440.
- Filippenko, A.V., 1997. Optical Spectra of Supernovae. *Annu Rev Astron Astrophys* 35, 309–355. doi:10.1146/annurev.astro.35.1.309.
- Fitzpatrick, E.L., 1999. Correcting for the Effects of Interstellar Extinction. *Publ Astron Soc Pac* 111, 63–75. doi:10.1086/316293, arXiv:astro-ph/9809387.
- Gal-Yam, A., Arcavi, I., Ofek, E.O., Ben-Ami, S., Cenko, S.B., Kasliwal, M.M., Cao, Y., Yaron, O., Tal, D., Silverman, J.M., Horesh, A., De Cia, A., Taddia, F., Sollerman, J., Perley, D., Vreeswijk, P.M., Kulkarni, S.R., Nugent, P.E., Filippenko, A.V., Wheeler, J.C., 2014. A Wolf-Rayet-like progenitor of SN 2013cu from spectral observations of a stellar wind. *Nature* 509, 471–474. doi:10.1038/nature13304, arXiv:1406.7640.
- Galbany, L., Hamuy, M., Phillips, M.M., Suntzeff, N.B., Maza, J., de Jaeger, T., Moraga, T., González-Gaitán, S., Krisciunas, K., Morrell, N.I., Thomas-Osip, J., Krzeminski, W., González, L., Antezana, R., Wishniewski, M., McCarthy, P., Anderson, J.P., Gutiérrez, C.P., Stritzinger, M., Folatelli, G., Anguita, C., Galaz, G., Green, E.M., Impey, C., Kim, Y.C., Kirhakos, S., Malkan, M.A., Mulchaey, J.S., Phillips, A.C., Pizzella, A., Prosser, C.F., Schmidt, B.P., Schommer, R.A., Sherry, W., Strolger, L.G., Wells, L.A., Williger, G.M., 2016. UBVR_{Iz} Light Curves of 51 Type II Supernovae. *Astron J* 151, 33. doi:10.3847/0004-6256/151/2/33, arXiv:1511.08402.
- Hiramatsu, D., Howell, D.A., Van Dyk, S.D., Goldberg, J.A., Maeda, K., Moriya, T.J., Tominaga, N., Nomoto, K., Hosseinzadeh, G., Arcavi, I., McCully, C., Burke, J., Bostroem, K.A., Valenti, S., Dong, Y., Brown, P.J., Andrews, J.E., Bilinski, C., Williams, G.G., Smith, P.S., Smith, N., Sand, D.J., Anand, G.S., Xu, C., Filippenko, A.V., Bersten, M.C., Folatelli, G., Kelly, P.L., Noguchi, T., Itagaki, K., 2021. The electron-capture origin of supernova 2018zd. *Nature Astronomy* 5, 903–910. doi:10.1038/s41550-021-01384-2, arXiv:2011.02176.
- Honscheid, K., DePoy, D.L., 2008. The Dark Energy Camera (DECam). *arXiv e-prints*, arXiv:0810.3600doi:10.48550/arXiv.0810.3600, arXiv:0810.3600.
- Hoogendam, W., Auchettl, K., Tucker, M., Ashall, C., Shappee, B., Huber, M., 2024. Early Spectrum of SN 2024ggi from SCAT shows a Type II SN with Flash Ionized Features. *Transient Name Server AstroNote* 103, 1.
- Hosseinzadeh, G., Bostroem, K.A., Gomez, S., 2023a. Light Curve Fitting. doi:10.5281/zenodo.8049154.
- Hosseinzadeh, G., Farah, J., Shrestha, M., Sand, D.J., Dong, Y., Brown, P.J., Bostroem, K.A., Valenti, S., Jha, S.W., Andrews, J.E., Arcavi, I., Haislip, J., Hiramatsu, D., Hoang, E., Howell, D.A., Janzen, D., Jencson, J.E., Kouprianov, V., Lundquist, M., McCully, C., Meza Retamal, N.E., Modjaz, M., Newsome, M., Padilla Gonzalez, E., Pearson, J., Pellegrino, C., Ravi, A.P., Reichart, D.E., Smith, N., Terreran, G., Vinkó, J., 2023b. Shock Cooling and Possible Precursor Emission in the Early Light Curve of the Type II SN 2023ixf. *Astrophys Jour Lett* 953, L16. doi:10.3847/2041-8213/ace4c4, arXiv:2306.06097.
- Hosseinzadeh, G., Sand, D.J., Valenti, S., Brown, P., Howell, D.A., McCully, C., Kasen, D., Arcavi, I., Bostroem, K.A., Tartaglia, L., Hsiao, E.Y., Davis, S., Shahbandeh, M., Stritzinger, M.D., 2017. Early Blue Excess from the Type Ia Supernova 2017cbv and Implications for Its Progenitor. *Astrophys Jour Lett* 845, L11. doi:10.3847/2041-8213/aa8402, arXiv:1706.08990.
- Huang, B., Yuan, H., Xiang, M., Huang, Y., Xiao, K., Xu, S., Zhang, R., Yang, L., Niu, Z., Gu, H., 2024. A Comprehensive Correction of the Gaia DR3 XP Spectra. *Astrophys Jour Suppl* 271, 13. doi:10.3847/1538-4365/ad1801, arXiv:2401.12006.
- Itagaki, K., 2023. Transient Discovery Report for 2023-05-19. *Transient Name Server Discovery Report* 2023-1158, 1.
- Jacobson-Galán, W.V., Davis, K.W., Kilpatrick, C.D., Dessart, L., Margutti, R., Chornock, R., Foley, R.J., Arunachalam, P., Auchettl, K., Bom, C.R., Cartier, R., Coulter, D.A., Dimitriadis, G., Dickinson, D., Drout, M.R., Gagliano, A.T., Gall, C., Garretson, B., Izzo, L., Jones, D.O., LeBaron, N., Miao, H.Y., Milisavljevic, D., Pan, Y.C., Rest, A., Rojas-Bravo, C., Santos, A., Sears, H., Subrayan, B.M., Taggart, K., Tinyanont, S., 2024. SN 2024ggi in NGC 3621: Rising Ionization in a Nearby, CSM-Interacting Type II Supernova. *arXiv e-prints*, arXiv:2404.19006doi:10.48550/arXiv.2404.19006, arXiv:2404.19006.
- Jencson, J.E., Pearson, J., Beasor, E.R., Lau, R.M., Andrews, J.E., Bostroem, K.A., Dong, Y., Engesser, M., Gomez, S., Guo, M., Hoang, E., Hosseinzadeh, G., Jha, S.W., Karambelkar, V., Kasliwal, M.M., Lundquist, M., Meza Retamal, N.E., Rest, A., Sand, D.J., Shahbandeh, M., Shrestha, M., Smith, N., Strader, J., Valenti, S., Wang, Q., Zenati, Y., 2023. A Luminous Red Supergiant and Dusty Long-period Variable Progenitor for SN 2023ixf. *Astrophys Jour Lett* 952, L30. doi:10.3847/2041-8213/ace618, arXiv:2306.08678.
- Killestein, T., Ackley, K., Kotak, R., O'Neill, D., Ramsay, G., Steeghs, D., Pursiainen, M., Dyer, M., Jiménez-Ibarra, F., Lyman, J., Ulaczyk, K., Galloway, D., Dhillon, V., O'Brien, P., Noysena, K., Breton, R., Nuttall, L., Pallé, E., Pollacco, D., Kumar, A., O'Neill, D., Jarvis, D., 2024. AT2024ggi: confirmation of an infant transient at 7 Mpc and improved constraint on explosion epoch. *Transient Name Server AstroNote* 101, 1.
- Kilpatrick, C.D., Foley, R.J., Jacobson-Galán, W.V., Piro, A.L., Smartt, S.J., Drout, M.R., Gagliano, A., Gall, C., Hjorth, J., Jones, D.O., Mandel, K.S., Margutti, R., Ramirez-Ruiz, E., Ransome, C.L., Villar, V.A., Coulter, D.A., Gao, H., Matthews, D.J., Taggart, K., Zenati, Y., 2023. SN 2023ixf in Messier 101: A Variable Red Supergiant as the Progenitor Candidate to a Type II Supernova. *Astrophys Jour Lett* 952, L23. doi:10.3847/2041-8213/ace4ca, arXiv:2306.04722.
- Li, G., Hu, M., Li, W., Yang, Y., Wang, X., Yan, S., Hu, L., Zhang, J., Mao, Y., Riise, H., Gao, X., Sun, T., Liu, J., Xiong, D., Wang, L., Mo, J., Iskandar, A., Xi, G., Xiang, D., Wang, L., Sun, G., Zhang, K., Chen, J., Lin, W., Guo, F., Liu, Q., Cai, G., Zhou, W., Zhao, J., Chen, J., Zheng, X., Li, K., Zhang, M., Xu, S., Lyu, X., Castro-Tirado, A.J., Chufarin, V., Potapov, N., Ionov, I., Korotkiy, S., Nazarov, S., Sokolovsky, K., Hamann, N., Herman, E., 2024. A shock flash breaking out of a dusty

- red supergiant. *Nature* 627, 754–758. doi:10.1038/s41586-023-06843-6, arXiv:2311.14409.
- Liu, C., Chen, X., Er, X., Zeimann, G.R., Vinkó, J., Wheeler, J.C., Cooper, E.M., Davis, D., Farrow, D.J., Gebhardt, K., Guo, H., Hill, G.J., House, L., Kollatschny, W., Kong, F., Kumar, B., Liu, X., Tuttle, S., Endl, M., Duke, P., Cochran, W.D., Zhang, J., Liu, X., 2023. The Preexplosion Environments and the Progenitor of SN 2023ixf from the Hobby-Eberly Telescope Dark Energy Experiment (HETDEX). *Astrophys Jour Lett* 958, L37. doi:10.3847/2041-8213/ad0da8, arXiv:2311.10400.
- Margutti, R., Grefenstette, B., 2024. NuSTAR detection of SN2024ggi at 2 days post discovery. *The Astronomer's Telegram* 16587, 1.
- Martinez, L., Bersten, M.C., Anderson, J.P., Hamuy, M., González-Gaitán, S., Förster, F., Orellana, M., Stritzinger, M., Phillips, M.M., Gutiérrez, C.P., Burns, C., Contreras, C., de Jaeger, T., Ertini, K., Folatelli, G., Galbany, L., Höflich, P., Hsiao, E.Y., Morrell, N., Pessi, P.J., Suntzeff, N.B., 2022. Type II supernovae from the Carnegie Supernova Project-I. II. Physical parameter distributions from hydrodynamical modelling. *Astron Astrophys* 660, A41. doi:10.1051/0004-6361/202142076, arXiv:2111.06529.
- Moriya, T.J., Förster, F., Yoon, S.C., Gräfener, G., Blinnikov, S.I., 2018. Type IIP supernova light curves affected by the acceleration of red supergiant winds. *Mon Not R Astron Soc* 476, 2840–2851. doi:10.1093/mnras/sty475, arXiv:1802.07752.
- Morozova, V., Piro, A.L., Valenti, S., 2018. Measuring the Progenitor Masses and Dense Circumstellar Material of Type II Supernovae. *Astrophys Jour* 858, 15. doi:10.3847/1538-4357/aa9a6, arXiv:1709.04928.
- Nicholl, M., 2018. SuperBol: A User-friendly Python Routine for Bolometric Light Curves. *Res. Notes Am. Astron. Soc.* 2, 230. doi:10.3847/2515-5172/aaf799.
- Pérez-Fournon, I., Poidevin, F., Aguado, D.S., Acosta-Pulido, J.A., López-Oramas, A., Nespral, D., 2024. Identification of the likely progenitor star of SN 2024ggi in the near IR with the VISTA Hemisphere Survey. *Transient Name Server AstroNote* 107, 1.
- Pessi, T., et al., 2024. Early flash-ionization lines in SN 2024ggi revealed by high-resolution spectroscopy. *arXiv e-prints*, arXiv:2405.02274doi:2405.02274/arXiv.2405.02274, arXiv:2405.02274.
- Quimby, R.M., Wheeler, J.C., Höflich, P., Akerlof, C.W., Brown, P.J., Rykoff, E.S., 2007. SN 2006bp: Probing the Shock Breakout of a Type II-P Supernova. *Astrophys Jour* 666, 1093–1107. doi:10.1086/520532, arXiv:0705.3478.
- Rabinak, I., Waxman, E., 2011. The Early UV/Optical Emission from Core-collapse Supernovae. *Astrophys Jour* 728, 63. doi:10.1088/0004-637X/728/1/63, arXiv:1002.3414.
- Schlafly, E.F., Finkbeiner, D.P., 2011. Measuring Reddening with Sloan Digital Sky Survey Stellar Spectra and Recalibrating SFD. *Astrophys Jour* 737, 103. doi:10.1088/0004-637X/737/2/103, arXiv:1012.4804.
- Smartt, S.J., 2009. Progenitors of Core-Collapse Supernovae. *Annu Rev Astron Astrophys* 47, 63–106. doi:10.1146/annurev-astro-082708-101737, arXiv:0908.0700.
- Smartt, S.J., 2015. Observational Constraints on the Progenitors of Core-Collapse Supernovae: The Case for Missing High-Mass Stars. *Publ of the Astron Soc of Australia* 32, e016. doi:10.1017/pasa.2015.17, arXiv:1504.02635.
- Soraisam, M.D., Szalai, T., Van Dyk, S.D., Andrews, J.E., Srinivasan, S., Chun, S.H., Matheson, T., Scicluna, P., Vasquez-Torres, D.A., 2023. The SN 2023ixf Progenitor in M101. I. Infrared Variability. *Astrophys Jour* 957, 64. doi:10.3847/1538-4357/acef22, arXiv:2306.10783.
- Srivastav, S., Chen, T.W., Smartt, S.J., Nicholl, M., Smith, K.W., Young, D.R., Fulton, M., McCollum, M., Moore, T., Weston, J., Sheng, X., Aamer, A., Angus, C.R., Ramsden, P., Shingles, L., Gillanders, J., Rhodes, L., Andersson, A., Stevance, H., Denneau, L., Tonry, J., Weiland, H., Lawrence, A., Siverd, R., Erasmus, N., Koorts, W., Jordan, A., Suc, V., Rest, A., Stubbs, C., Sommer, J., 2024. ATLAS24fsk (AT2024ggi): discovery of a nearby candidate SN in NGC 3621 at 7 Mpc with a possible progenitor detection. *Transient Name Server AstroNote* 100, 1.
- Steeghs, D., Galloway, D.K., Ackley, K., Dyer, M.J., Lyman, J., Ulaczyk, K., Cutter, R., Mong, Y.L., Dhillon, V., O'Brien, P., Ramsay, G., Poshyachinda, S., Kotak, R., Nuttall, L.K., Pallé, E., Breton, R.P., Pollacco, D., Thrane, E., Aukkaravitayapun, S., Awiphan, S., Burhanudin, U., Chote, P., Chrimes, A., Daw, E., Duffy, C., Eyles-Ferris, R., Gompertz, B., Heikkilä, T., Irawati, P., Kennedy, M.R., Killestein, T., Kuncarayakti, H., Levan, A.J., Littlefair, S., Makrygianni, L., Marsh, T., Mata-Sanchez, D., Mattila, S., Maund, J., McCormac, J., Mkrtchian, D., Mullaney, J., Noysena, K., Patel, M., Rol, E., Sawangwit, U., Stanway, E.R., Starling, R., Strøm, P., Tooke, S., West, R., White, D.J., Wiersema, K., 2022. The Gravitational-wave Optical Transient Observer (GOTO): prototype performance and prospects for transient science. *Mon Not R Astron Soc* 511, 2405–2422. doi:10.1093/mnras/stac013, arXiv:2110.05539.
- Tartaglia, L., Fraser, M., Sand, D.J., Valenti, S., Smartt, S.J., McCully, C., Anderson, J.P., Arcavi, I., Elias-Rosa, N., Galbany, L., Gal-Yam, A., Haislip, J.B., Hosseinzadeh, G., Howell, D.A., Inserra, C., Jha, S.W., Kankare, E., Lundqvist, P., Maguire, K., Mattila, S., Reichart, D., Smith, K.W., Smith, M., Stritzinger, M., Sullivan, M., Taddia, F., Tomasella, L., 2017. The Progenitor and Early Evolution of the Type IIb SN 2016gkg. *Astrophys Jour Lett* 836, L12. doi:10.3847/2041-8213/aa5c7f, arXiv:1611.00419.
- Teja, R.S., Singh, A., Basu, J., Anupama, G.C., Sahu, D.K., Dutta, A., Swain, V., Nakaoka, T., Pathak, U., Bhalerao, V., Barway, S., Kumar, H., A. J., N., Imazawa, R., Kumar, B., Kawabata, K.S., 2023. Far-ultraviolet to Near-infrared Observations of SN 2023ixf: A High-energy Explosion Engulfed in Complex Circumstellar Material. *Astrophys Jour Lett* 954, L12. doi:10.3847/2041-8213/acef20, arXiv:2306.10284.
- Tonry, J., Denneau, L., Weiland, H., Lawrence, A., Siverd, R., Erasmus, N., Koorts, W., Jordan, A., Suc, V., Smartt, S.J., Smith, K.W., Young, D.R., Nicholl, M., Fulton, M., McCollum, M., Moore, T., Weston, J., Sheng, X., Ramsden, P., Angus, C.R., Aamer, A., Shingles, L., Srivastav, S., Gillanders, J., Rhodes, L., Andersson, A., Stevance, H., Rest, A., Chen, T.W., Stubbs, C., Sommer, J., 2024. ATLAS Transient Discovery Report for 2024-04-11. *Transient Name Server Discovery Report* 2024-1020, 1.
- Valenti, S., Howell, D.A., Stritzinger, M.D., Graham, M.L., Hosseinzadeh, G., Arcavi, I., Bildsten, L., Jerkstrand, A., McCully, C., Pastorello, A., Piro, A.L., Sand, D., Smartt, S.J., Terreran, G., Baltay, C., Benetti, S., Brown, P., Filippenko, A.V., Fraser, M., Rabinowitz, D., Sullivan, M., Yuan, F., 2016. The diversity of Type II supernova versus the similarity in their progenitors. *Mon Not R Astron Soc* 459, 3939–3962. doi:10.1093/mnras/stw870, arXiv:1603.08953.
- Wang, C.J., Bai, J.M., Fan, Y.F., Mao, J.R., Chang, L., Xin, Y.X., Zhang, J.J., Lun, B.L., Wang, J.G., Zhang, X.L., Ying, M., Lu, K.X., Wang, X.L., Ji, K.F., Xiong, D.R., Yu, X.G., Ding, X., Ye, K., Xing, L.F., Yi, W.M., Xu, L., Zheng, X.M., Feng, Y.J., He, S.S., Wang, X.L., Liu, Z., Chen, D., Xu, J., Qin, S.N., Zhang, R.L., Tan, H.S., Li, Z., Lou, K., Li, J., Liu, W.W., 2019. Lijiang 2.4-meter Telescope and its instruments. *Research in Astronomy and Astrophysics* 19, 149. doi:10.1088/1674-4527/19/10/149, arXiv:1905.05915.
- Waxman, E., Katz, B., 2017. Shock Breakout Theory, in: Alsabti, A.W., Murdin, P. (Eds.), *Handbook of Supernovae*. Springer International Publishing, p. 967. doi:10.1007/978-3-319-21846-5_33.
- Yang, S., Chen, T.W., Stevance, H.F., Smartt, S.J., Srivastav, S., Gillanders, J., Fulton, M., Moore, T., Smith, K.W., 2024. Maximum luminosity of the progenitor of SN 2024ggi (ATLAS24fsk) from the Legacy Survey images. *Transient Name Server AstroNote* 105, 1.
- Yaron, O., Perley, D.A., Gal-Yam, A., Groh, J.H., Horesh, A., Ofek, E.O., Kulkarni, S.R., Sollerman, J., Fransson, C., Rubin, A., Szabo, P., Sapir, N., Taddia, F., Cenko, S.B., Valenti, S., Arcavi, I., Howell, D.A., Kasliwal, M.M., Vreeswijk, P.M., Khazov, D., Fox, O.D., Cao, Y., Gnat, O., Kelly, P.L., Nugent, P.E., Filippenko, A.V., Laher, R.R., Woźniak, P.R., Lee, W.H., Rebba-pragada, U.D., Maguire, K., Sullivan, M., Soumagnac, M.T., 2017. Confined dense circumstellar material surrounding a regular type II supernova. *Nature Physics* 13, 510–517. doi:10.1038/nphys4025, arXiv:1701.02596.
- Zhai, Q., Li, L., Wang, Z., Zhang, J., Wang, X., 2024. LJT spectroscopic classification of AT 2024ggi as a young Type II supernova with flash features. *Transient Name Server AstroNote* 104, 1.

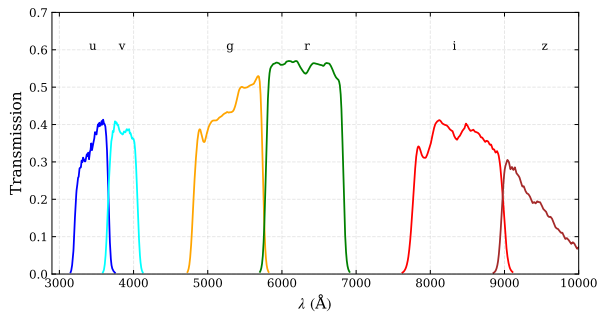


Figure 7: The transmission curves of the six filters adopted by the Mephisto telescope.

Zhang, J., Li, C.K., Cheng, H.Q., Wu, Q.Y., Jia, S.M., Chen, Y., Cui, W.W., Feng, H., Guan, J., Han, D.W., Li, W., Liu, C.Z., Lu, F.J., Song, L.M., Wang, J., Xu, J.J., Zhang, S.N., Zhao, H.S., Zhao, X.F., Jin, C.C., Ling, Z.X., Liu, H.Y., Liu, M.J., Liu, Y., Li, D.Y., Sun, H., Yuan, W., Zhang, C., Zhang, W.D., Li, R.Z., Wang, Y., Zhou, H., Nandra, K., Rau, A., Friedrich, P., Meidinger, N., Burwitz, V., Kuulkers, E., Santovincenzo, A., O'Brien, P., Cordier, B., Wang, X.F., Li, W.X., 2024. SN 2024ggi: detection of X-ray emission by EP-FXT. The Astronomer's Telegram 16588, 1.

Zhang, J., Lin, H., Wang, X., Zhao, Z., Li, L., Liu, J., Yan, S., Xiang, D., Wang, H., Bai, J., 2023. Circumstellar material ejected violently by a massive star immediately before its death. Science Bulletin 68, 2548–2554. doi:[10.1016/j.scib.2023.09.015](https://doi.org/10.1016/j.scib.2023.09.015), arXiv:2309.01998.

Zhang, J., Wang, X., József, V., Zhai, Q., Zhang, T., Filippenko, A.V., Brink, T.G., Zheng, W., Wyrzykowski, Ł., Mikolajczyk, P., Huang, F., Rui, L., Mo, J., Sai, H., Zhang, X., Wang, H., DerKacy, J.M., Baron, E., Sárneczky, K., Bódi, A., Csörnyei, G., Hanyecz, O., Ignácz, B., Kalup, C., Kriskovics, L., Könyves-Tóth, R., Ordasi, A., Pál, A., Sódor, Á., Szakáts, R., Vida, K., Zsidi, G., 2020. SN 2018zd: an unusual stellar explosion as part of the diverse Type II Supernova landscape. Mon Not R Astron Soc 498, 84–100. doi:[10.1093/mnras/staa2273](https://doi.org/10.1093/mnras/staa2273), arXiv:2007.14348.

Zimmerman, E.A., Irani, I., Chen, P., Gal-Yam, A., Schulze, S., Perley, D.A., Sollerman, J., Filippenko, A.V., Shenar, T., Yaron, O., Shahaf, S., Bruch, R.J., Ofek, E.O., De Cia, A., Brink, T.G., Yang, Y., Vasylyev, S.S., Ben Ami, S., Aubert, M., Badash, A., Bloom, J.S., Brown, P.J., De, K., Dimitriadis, G., Fransson, C., Fremling, C., Hinds, K., Horesh, A., Johansson, J.P., Kasliwal, M.M., Kulkarni, S.R., Kushnir, D., Martin, C., Matuzewski, M., McGurk, R.C., Miller, A.A., Morag, J., Neil, J.D., Nugent, P.E., Post, R.S., Prusinski, N.Z., Qin, Y., Raichoor, A., Riddle, R., Rowe, M., Rusholme, B., Sfaradi, I., Sjoberg, K.M., Soumagnac, M., Stein, R.D., Strotjohann, N.L., Terwel, J.H., Wasserman, T., Wise, J., Wold, A., Yan, L., Zhang, K., 2023. Resolving the explosion of supernova 2023ixf in Messier 101 within its complex circumstellar environment. arXiv e-prints , arXiv:2310.10727doi:[10.48550/arXiv.2310.10727](https://doi.org/10.48550/arXiv.2310.10727), arXiv:2310.10727.

A. Mephisto supporting facilities and filter transmission function

Along with 1.6m Mephisto there are two 50 cm auxiliary photometric telescopes at the site. The 50 cm array (model: Alluna RC20) has a 505 mm optical aperture and an f/8.1 focal ratio. Both are equipped with FLI ML 50100 CCD camera 8176×6132 pixels of (size $6 \mu\text{m}$). The filter systems on these facilities are the same so that coordinated observations can be easily performed (cf. transients detected with the 1.6m telescope). The $uvgriz$ transmission function is provided in Fig. 7.